NOTATION

t, time; T, temperature; r, radial coordinate; ℓ and R, pipe length and radius, ρ_1 and ρ_2, densities of frozen layer and liquid; c_1 and c_2, specific heats of frozen layer and liquid; λ, thermal conductivity of liquid; q, latent heat of phase transition; r_*, clear cross section radius; k_1, heat-transfer coefficient for frozen layer to environment; k_2, heat-transfer coefficient from flow to frozen zone; $\kappa = \lambda/\rho_1 c_1$, thermal diffusivity for frozen layer; $Re = 2wR/\nu$, Reynolds number; $Gr = 8R^3\xi g(T_1 - T_*)/\nu^3$, Grashof number; $Pr = \nu\rho_2 c_2/\lambda$, Prandtl number; ν, kinematic viscosity; w, flow speed; g, acceleration due to gravity; ξ, bulk expansion coefficient.

LITERATURE CITED

1. V. M. Agapkin, B. A. Krivoshein, and V. A. Yufin, Thermal and Hydraulic Calculations on Pipelines for Oil and Oil Products [in Russian], Moscow (1981).
2. N. M. Dubina and B. A. Krasovitskii, Heat Transfer and Interaction Mechanics with Soils for Pipelines and Boreholes [in Russian], Novosibirsk (1983).
3. Z. P. Shul'man, B. M. Khusid, and E. A. Zal'tsgendler, Heat Transfer in the Flow of a Heat-Sensitive Non-Newtonian Liquid in a Long Channel [in Russian], Preprint ITMO AN BSSR No. 22, Minsk (1982).
4. A. M. Stolin, S. I. Khudyaev, and S. V. Maklakov, Proceedings of the Seventh All-Union Heat and Mass Transfer Conference [in Russian], Vol. 5, Minsk (1984), pp. 145-152.
5. B. A. Krasovitskii, Inzh.-Fiz. Zh., 51, No. 5, 802-809 (1986).
6. C. O. Bennet and J. E. Myers, Hydrodynamics, Heat Transfer, and Mass Transfer [Russian translation], Moscow (1966).

EFFECTS OF WATER SPEED AND TEMPERATURE ON ICING IN THERMAL SIPHONS

P. A. Vislobitskii, V. M. Gorislavets, and A. G. Taran

UDC 536.421.4

A numerical study has been made on the freezing in a thermal siphon immersed in water with free or forced convection. The effects of various factors on the ice column diameter are examined.

In the construction of major pipelines in West Siberia, an important part is played by traverses through rivers, lakes, and lowland areas generally. There are persistent negative air temperatures, which are maintained for long periods in such places, which can give rise to ice or frozen-soil environments. However, the carrying capacity of such ice is usually insufficient to allow access to heavy vehicles or constructional machinery. To strengthen the load capacity of such crossings, one installs wooden structures and freezes the ice by means of thermal siphons.

A construction proposed in [1] for an ice crossing with frozen cylindrical columns can reduce the time and cost of construction and increase the load capacity, particularly if the underlying ground is soft.

One begins to install such ice bridges after a continuous ice sheet 10-15 cm thick has formed naturally. The evaporative parts of the siphons are inserted through holes drilled in the ice cover, which extend into the underlying soil. When the ice columns are formed, the soil is also frozen around the buried part of the siphon. The frozen soil provides a reliable base for the ice column and does not yield. Such ice columns in ice crossings can be used on winter vehicle roads and can increase the load capacity of the ice cover by a factor 1.5-2.

The freezing around a siphon is determined mainly by the surrounding air temperature, the water temperature, and the wind and water speeds. The availability of a structure for

All-Union Institute for Research on Constructing Major Pipelines, Kiev Branch.

Translated from Inzhenerno-Fizicheskii Zhurnal, Vol. 54, No. 6, pp. 942-949, June, 1988. Original article submitted April 13, 1987.

0022-0841/88/5406-0629$12.50

© 1988 Plenum Publishing Corporation

use is judged from the diameter of the frozen column, i.e., it is necessary to know how the relative diameter varies with time. This is determined from the heat-transfer treatment for the part of the siphon immersed in the water and the surrounding water.

It is assumed that at the start, the temperature at the outer surface of the underwater part of the siphon is equal to that of the surrounding water. As the siphon cools, the surface temperature falls and eventually becomes negative. A layer of ice is formed, which gradually thickens. It is assumed that the mobile boundary in contact with the water is always at the transition temperature. The latent heat of fusion is released at this boundary, and this is transmitted by conduction through the ice to the siphon. The immobile boundary at the surface has the outside temperature of the siphon, which varies with time.

It is also assumed that the thermophysical parameters in the two phases are different but are constant for each phase, and that the phase transition occurs completely at temperature T_f, which is taken as constant, with the heat transferred from the water to the transition front by natural convection if the water is stationary or forced if it is flowing.

The problem is that of setting in a homogeneous isotropic medium around a cooled cylinder subject to boundary conditions of the third kind at the surface and at the phase boundary:

$$\frac{\partial T_1(r,\ t)}{\partial t} = \frac{a_1}{r}\frac{\partial}{\partial r}\left(r\frac{\partial T_1(r,\ t)}{\partial r}\right), r_0 \leqslant r \leqslant r_f,\ t \geqslant t_f. \tag{1}$$

$$\lambda_1 \frac{\partial T_1(r,\ t)}{\partial r}\bigg|_{r=r_f} = \alpha_f (T_{wa} - T_f) + \gamma_2 L \frac{dr_f}{dt}. \tag{2}$$

$$T_1(r_f,\ t) = T_f = \text{const}. \tag{3}$$

$$\lambda_1 \frac{\partial T_1(r_f,\ t)}{\partial r}\bigg|_{r=r_0} = k(T_w(t) - T_a). \tag{4}$$

$$T_2(r > r_f,\ t) = T_2(r,\ 0) = T_{wa}. \tag{5}$$

This system shows that the internal sink in the siphon is not considered, since it has little influence on the effective heat-transfer coefficient for a vapor siphon [2]. The siphon action is incorporated as an effective resistance between the air and the outer surface of the underwater part of the siphon, where the vapor siphon has that resistance determined in the main by the heat-transfer coefficient between the air and the outer surface in the condenser part.

The reduced heat-transfer coefficient is [3] defined as

$$k_{re} \simeq \xi \frac{F_c}{F_e}\alpha_a, \tag{6}$$

Here ξ incorporates the resistance within the siphon and is dependent on the type and design. In general, one can say that $0.2 < \xi < 0.5$ for the liquid siphon and $\xi > 0.8$ for a vapor one. In our calculations, $k_{re} \simeq \alpha_a$, i.e., it is assumed that the surface area F_e of the evaporative (underwater) part and the area F_c for the condenser (air) part are identical, and ξ is taken as 1.

Unfortunately, α_a is variable, and the error of measurement is about 25%. To calculate it, one needs to consider the radiative component as well as the convective one, as well as the scope for variation in fin performance with wind direction. In our calculations, we took k = 50 W/m^2·deg as very good, since our purpose was to determine the siphon freezing aureole under the most favorable conditions. Under field conditions, α_a is in the range from 6 to 50 W/m^2·deg, so to incorporate the effects of α_a on the performance, we simultaneously made calculations for k = 12.5 W/m^2·deg, which was considered a satisfactory value.

Particular attention was also given to choosing the value for the heat-transfer coefficient α_f from the water to the frozen layer, or the Nusselt number. There is almost no published information on α_f for tube icing. If a tube is iced with forced convection, one

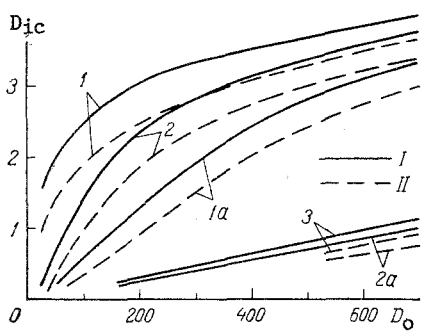

Fig. 1

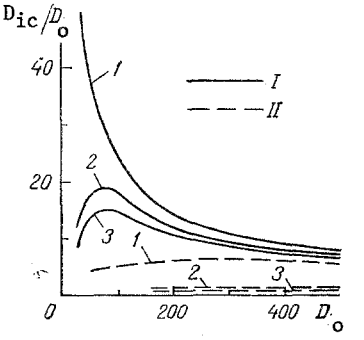

Fig. 2

Fig. 1. Frozen column diameter as a function of siphon diameter: 1) stagnant water, T_{wa} = 0.05°C; 1a) stagnant water, T_{wa} = 4°C; 2) flow speed 1.8 kg/h, T_{wa} = 0.05°C; 2a) flow speed 1.8 km/h, T_{wa} = 4°C; 3) flow speed 1 km/h, T_{wa} = 4°C; I) k = 50 W/m²·deg; II) 12.5. D_{ic} in m, D_o in mm.

Fig. 2. Relative diameter of frozen column as a function of siphon diameter for k = 50 W/m²·deg: 1) stagnant water; 2) flow speed 1 km/h; 3) flow speed 1.8 km/h; I) T_{wa} = 0.05°C; II) 4°C.

can take the corresponding Nusselt number from [4], where measurements were made on Nu as a function of the Reynolds number for moist air blown around a cylinder cooled to low temperatures. The Nusselt numbers taken from [4] were 55 and 76 for flow speeds of 1.0 and 1.8 km/h correspondingly.

For column freezing in stagnant water, the Nusselt number as a function of water temperature was determined from [5], which dealt with thawing in ice spheres in stagnant water at various temperatures. To check the scope for using the [5] data under tube freezing conditions, estimates were made [6] on α_f from measurements on freezing for a tube transporting cold air in stagnant water. The Nu(T) graph given in [5] is suitable for calculating tube freezing with natural convection, as it gives the Nusselt number for water temperatures of 1 and 4°C as 4, while Nu ≈ 7 for water temperatures of 2 and 3°C. If the water temperature is close to zero (0.05°C), the Nusselt number can be taken as approximately 2.

A numerical method was applied directly to (1)-(5), where the following dimensionless quantities were used:

$$U = \frac{T_1 - T_f}{T_f - T_a};\ V_0 = \frac{\lambda_2}{\lambda_1}\frac{T_{wa} - T_f}{T_f - T_a};\ \tau = \frac{a_1 t}{r_o^2};$$
$$\mathrm{Bi} = \frac{k r_o}{\lambda_1};\ \mathrm{Nu} = \frac{2\alpha_f r_o}{\lambda_2};\ R = \ln(r/r_o). \tag{7}$$

A finite-difference method was employed [7] with an inexplicit scheme but explicit phase-boundary identification. The region outside the siphon was covered by a uniform net, step h. It was assumed that at any given instant, one knows $R_f = R_f(\tau)$ and the temperatures

$$U_n = U(\tau,\ nh),\ n = 0,\ 1,\ \ldots,\ N. \tag{8}$$

The phase boundary at each successive instant is determined as

$$\hat{R}_f = R_f + \Delta R_f, \tag{9}$$

with ΔR_f defined by

$$\Delta R_f = \frac{C_1 (T_f - T_a)\Delta\tau}{L \exp(2R_f)}\frac{\gamma_1}{\gamma_2}\left[\left(\frac{\partial U}{\partial R}\right)_{R=R_f} - \frac{\mathrm{Nu} V_0}{2}\exp(R_f)\right]. \tag{2a}$$

Here (2a) contains a partial derivative, which was approximated as

$$\left.\frac{\partial U}{\partial R}\right|_{R=R_f} = -\frac{(4h+\delta)(3h+\delta)}{6(h+\delta)h^3}U_{m-1} + \frac{(4h+\delta)(3h+\delta)(h+\delta)}{2(2h+\delta)h^3}U_{m-2} -$$

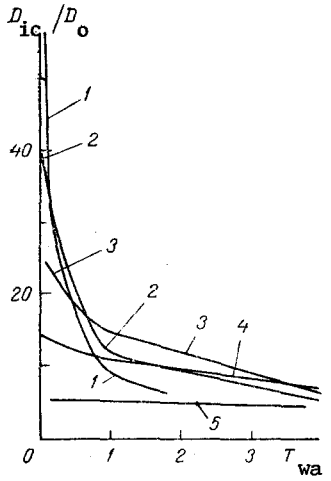

Fig. 3

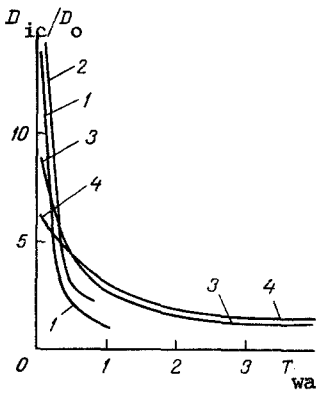

Fig. 4

Fig. 3. Relative ice diameter as a function of water temperature with free convection for k = 50 W/m²·deg: 1) D_o = 25 mm; 2) 50; 3) 102; 4) 219; 5) 700. T_{wa}, °C.

Fig. 4. Relative ice diameter as a function of water temperature for a flow speed of 1.8 km/h (k = 50 W/m²·deg): 1) D_o = 50 mm; 2) 102; 3) 325; 4) 530.

$$-\frac{(4h+\delta)(2h+\delta)(h+\delta)}{2(3h+\delta)h^3}U_{m-3}+\frac{(3h+\delta)(2h+\delta)(h+\delta)}{6(4h+\delta)h^3}U_{m-4}, \tag{10}$$

which is obtained by differentiating a five-point Lagrange interpolation formula [8], which enables one to calculate the temperature at an intermediate point from the known temperatures at the interpolation nodes m − 1, m − 2, m − 3, and m − 4 followed by substituting the U_m defined by that formula for $R = R_f$ (index m denotes the grid line in the frozen zone directly adjoining the phase boundary, while $\delta = R_f - R_m$ characterizes the distance between the phase boundary and the grid line m).

When the phase-transition front intersects the following grid line, m is redefined as m + 1.

As ΔR_f may be substantial, we determined the increment in the phase-transition radius from the time-averaged value $\bar{R}_f$, which was taken as R_f at time τ plus the increment in the phase-transition radius during the previous time step, i.e.,

$$\bar{R}_f = R_f + \Delta\check{R}_f/2, \tag{11}$$

where $\Delta\check{R}_f = R_f - \check{R}_f$.

When $\hat{R}_f$ has been calculated and $\hat{m}$ has been determined such that $\hat{m}h \leq \hat{R}_f \leq (\hat{m}+1)h$, we derive $\hat{U}_n$ by approximating (1) with a finite-difference inexplicit scheme

$$\frac{\hat{U}_n - U_n}{\tau} = \frac{a_1}{h^2}(\hat{U}_{n-1} - 2\hat{U}_n + \hat{U}_{n+1})\exp(-2R_n) \tag{12}$$

for all n = 1, 2, ..., $\hat{m}$ − 1 and also for n = $\hat{m}$ if $\hat{\delta} = \hat{R}_f - \hat{m}h = 0$. If on the other hand $\hat{\delta} > 0$, (12) for n = $\hat{m}$ is supplemented with

$$\frac{\hat{U}_{\hat{m}} - U_{\hat{m}}}{\tau} = \frac{2}{h+\delta}\left(-\frac{\hat{U}_{\hat{m}}}{\delta} - \frac{\hat{U}_{\hat{m}} - U_{\hat{m}-1}}{h}\right)\exp(-2R_{\hat{m}}). \tag{13}$$

Boundary condition (4) is approximated as

$$\frac{\hat{U}_1 - \hat{U}_0}{h} = h\frac{\hat{U}_0 - U_0}{2\tau} + \mathrm{Bi}(\hat{U}_0 + 1), \tag{14}$$

and (5) is represented exactly:

$$\hat{U}_n = V_0,\ n = \hat{m}+1,\ \ldots,\ N. \tag{15}$$

Difference scheme (12)-(15) was solved by the pivot method, which gave $\hat{U}_n$ for n = 0, 1, ..., N. We performed calculations for water temperatures of 0.05, 0.5, 1, 2, and 4°C. As regards obtaining the largest ice columns, the main interest attaches to the lowest air temperatures, so all the calculations were performed for an air temperature of −30°C for a wide range of tube diameters from 25 to 720 mm inclusive for free and forced convection. In the last case, we considered flow speeds of 1.0 and 1.8 km/h. The thermophysical parameters for ice and water were taken from [9].

In all cases, we considered a 180-day period in the calculations. All the thickness curves had the same characteristics: initially, the thickness increased rapidly, but then the growth rate slowed, and finally it ceased entirely. The time at which growth ceased was dependent on the water temperature and speed, as well as on the siphon diameter and performance.

The layer thinned as the water temperature increased; there was a similar effect from the flow speed. At a water temperature of 1°C, siphons with diameters 25, 50, and 76 mm with free convection gave the limiting ice thicknesses after 20, 80, 130 days correspondingly (for k = 50 W/m^2·deg) or at 10, 60, and 80 days for k = 12.5 W/m^2·deg. At 4°C, a 25-mm diameter siphon did not freeze, while the limiting ice thicknesses for 50 and 76 mm were attained in 10, 20 days correspondingly for k = 50 W/m^2·deg. Under these conditions, siphons with diameters 102, 159, and 219 mm reached the limit. With forced convection, the effects were much more pronounced. At 1 km/h, even a temperature of 0.05°C, i.e., close to zero, showed small siphons (25 and 50 mm diameter) reaching their limits rapidly, while at 0.5°C, the limits were quite rapidly reached with 76, 102, 159, 219, and 325 mm. At 1°C, there was virtually no ice on siphons less than 102 mm in diameter, while at 4°C, the limits were reached very rapidly for all diameters and the thickness was much reduced (by a factor 2.5-3 by comparison with stagnant water for diameters over 530 mm or by about a factor four for ones between 530 and 159 mm). This confirms that convection prevents the setting from continuing indefinitely, as is the case in transfer by conduction, and that freezing ceases after a finite time, because the amount of heat transmitted through the frozen layer by conduction decreases as the layer thickens, while the amount of heat brought up by convection increases with r_f [10]. Equilibration sets in at a certain instant and the freezing ceases. The larger the diameter, the later that state sets in, so particular care is needed in forecasting freezing for small-diameter siphons.

Figures 1-4 show calculations, with Fig. 1 showing the ice diameter as a function of underwater siphon diameter. The effective heat-transfer coefficient has a marked influence. The effects from siphon diameter decrease as the water temperature rises, particularly for running water. At 0.5 m/sec and 4°C, a diameter of over 500 mm is required to freeze the water, which is useless. Figure 2 shows the relative ice diameter as a function of siphon diameter. When the water temperature is close to zero and there is free convection, the relative diameter falls continuously as the siphon diameter increases, while in running water, there is a peak for diameters in the range 10-100 mm. At 4°C, the siphon diameter has virtually no effect on D_{ic}/D_o.

Figure 3 shows the ratio of the ice diameter to the siphon diameter as a function of water temperature for free convection; D_{ic}/D_o decreases as the temperature increases, and the less the siphon diameter, the more rapid the decrease. The largest fall in D_{ic}/D_o occurs in the range 0.05-1°C, after which the curves level out. Figure 4 shows the same relationship but for forced convection. There is an appreciable reduction in D_{ic}/D_o by comparison with Fig. 3. For siphon diameters 50-100 mm, D_{ic}/D_o differ by almost an order of magnitude between free and forced convection.

This program has been used to design ice crossings frozen by means of siphons in constructing major pipelines [11]. The reliability has been confirmed indirectly in strength tests. The method of calculating strength for ice bridges described in [11] takes the ice cover thickness as part of the input data, together with the water depth, the elastic and strength parameters for ice, and the ice column diameter and pitch. The diameter has been calculated by our method from the water temperature, flow speed, and mean air temperature in the period from the installation of the siphon to bridge loading. The calculations are highly reliable and thus support the methods used in calculating the load capacity. For a period of eight years since the industrial use of these ice crossings strengthened by ice columns, there has been no instance of damage during use.

NOTATION

T_1, C_1, a_1, λ_1, γ_1, solid-phase temperature, specific heat, thermal diffusivity, thermal conductivity, and density; T_2, λ_2, γ_2, liquid temperature, thermal conductivity, and density; r_o, siphon outside radius; D_o, siphon outside diameter; r_f, radius of phase transition front; D_{ic}, ice column diameter; k, effective siphon heat-transfer coefficient; T_a, T_{wa}, T_w, air temperature, water temperature around evaporative part, and temperature at outer surface of siphon correspondingly; T_f, phase-transition temperature; α_f, heat-transfer coefficient from water to phase-transition surface; L, latent heat of fusion; t_f, time required to produce ice of a given thickness on a siphon.

LITERATURE CITED

1. P. A. Vislobitskii, A. P. Klimenko, A. I. Titarenko, and Yu. N. Shirikhin, Stroit. Trubopr., No. 2, 29-30 (1982).
2. E. S. Kurylev, V. V. Onosovskii, and V. S. Sokolov, Kholodil'naya Tekh., No. 6, 37-41 (1974).
3. N. A. Buchko, I. K. Lebedkina, et al., Kholod. Tekh., No. 3, 25-27 (1976).
4. Hidetoshi Aoki et al., Ref. Zh. Mekh., No. 6, Ref. 7B 580 (1980).
5. J. M. Dumore et al., Nature, 172, No. 4375, 460-461 (1953).
6. V. M. Gorislavets and L. P. Semenov, Inzh.-Fiz. Zh., 48, No. 4, 610-617 (1985).
7. A. A. Samarskii, Introduction to Difference-Scheme Theory [in Russian], Moscow (1977).
8. P. F. Fil'chakov, Numerical and Graphical Methods in Applied Mathematics [in Russian], Kiev (1970).
9. A. V. Lykov, Thermal Conductivity Theory [in Russian], Moscow (1951).
10. E. M. Sparrow et al., Teploperedacha, No. 4, 1-9 (1979).
11. Instructions on Building Technology for Ice Crossings Frozen by Means of Two-Phase Thermal Siphons in the Construction of Major Pipelines [in Russian], VSN 175-84, Minneftegazstroi, Moscow (1985).

PROPERTIES OF NONSTEADY-STATE HEAT TRANSFER TO SUPERFLUID HELIUM

V. M. Miklyaev, I. A. Sergeev, and Yu. P. Filippov

UDC 536.48

Results are presented from an experimental study of heat transfer from a cylindrical specimen to a volume of superfluid helium with thermal loading in the form of an impulsive step. Unique features of He II as a cooling agent as compared to He I are noted and discussed.

In recent years the number of studies dedicated to heat transport and hydrodynamics of superfluid helium has increased significantly. This is due, first, to the need to construct an adequate heat transport theory [1], and second, to the possibility of practical use of He II as a cooling agent in cryogenic systems [2, 3]. In particular, the literature offers experimental data concerning the physics of the superfluid liquid (its hydrodynamics, acoustics, phase transitions) [4, 5] and processes occurring on a solid body–He II boundary (Kapitsa resistance, critical thermal flux, heat transport in various regimes) [6, 7]. However, as was noted in the review [1], questions of nonsteady state heat transfer to He II, the development of thermal perturbations with a turbulent front, and the dynamics of He II → He vapor and He II → He I phase transitions require additional study.

The goal of the present study is to investigate the processes of nonsteady-state heat transfer from the surface of a solid body of cylindrical form immersed in superfluid helium.

The experiments were performed in He II upon the free surface of which a pressure P_s = 1780 Pa was maintained (equilibrium temperature T_s = 1.82 K). The helium II volume ≈ $3.0 \cdot 10^{-3}$ m^3, the free liquid surface area ≈ $1.54 \cdot 10^{-2}$ m^2, specimen immersion depth 0.05-0.15 m.

Joint Institute for Nuclear Research, Dubna. Translated from Inzhenerno-Fizicheskii Zhurnal, Vol. 54, No. 6, pp. 950-956, June, 1988. Original article submitted February 6, 1987.

0022-0841/88/5406-0634$12.50

© 1988 Plenum Publishing Corporation